Bioconjugate Chemistry

Communication

pubs.acs.org/bc

Retargeting Polyomavirus-Like Particles to Cancer Cells by Chemical Modification of Capsid Surface

Jirina Zackova Suchanova,[†] Jitka Neburkova,[‡,§] Hana Spanielova,[†,‡] Jitka Forstova,[†] and Petr Cigler[‡]

[†]Department of Genetics and Microbiology, Faculty of Science, Charles University, Vinicna 5, 128 44 Prague 2, Czech Republic

[‡]Institute of Organic Chemistry and Biochemistry of the CAS, v.v.i., Flemingovo nam. 2, 166 10, Prague 6, Czech Republic

[§]First Faculty of Medicine, Charles University, Katerinska 32, 121 08, Prague 2, Czech Republic

Supporting Information

ABSTRACT: Virus-like particles based on polyomaviruses (PVLPs) are promising delivery devices for various cargoes, including nucleic acids, imaging probes, and therapeutic agents. In biological environments, the major coat protein VP1 interacts with ubiquitously distributed sialic acid residues, and therefore PVLPs show a broad tropism. For selective targeting, appropriate engineering of the PVLP surface is needed. Here, we describe a chemical approach to retarget PVLPs to cancer cells displaying abnormally high levels of transferrin receptor. We created an array of transferrin molecules on the surface of PVLPs by combining a high-yielding bioconjugation approach with specific point modification of transferrin. This artificial surface protein architecture enables (i) suppression of natural VP1-specific interactions by blocking the surface conformational epitope on the VP1 protein, (ii) unusually high cellular uptake efficiency, and (iii) selective retargeting of PVLPs to osteosarcoma (U2OS) and lymphoblastoid leukemia (CCRF-CEM) cells.

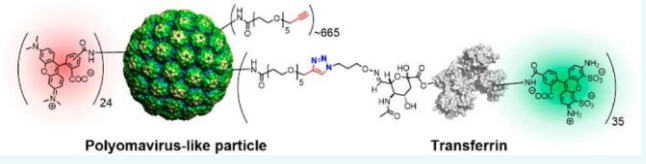

Virus-like particles (VLPs) have attracted considerable interest because of their potential bioapplications as ecient delivery vehicles. VLPs have an inherent capacity to interact with the cellular surface, enter cells, and release encapsulated content into cellular compartments.[1] Moreover, their highly symmetrical exteriors can serve as programmable scaffolds for further modifications, such as attaching multiple copies of a targeting moiety and achieving its high local concentration.[2]

Among these highly promising delivery devices are VLPs derived from the nonenveloped polyomaviruses (PVLPs),[3,4] which can be disassembled and reassembled in vitro and potentially used as nanocontainers for various cargoes, such as DNA,[5] RNA,[6] imaging probes,[7] and therapeutic agents.[8] PVLPs mainly consist of the major coat protein (VP1), which interacts with ubiquitously distributed sialic acid residues, giving PVLPs a naturally broad cell and tissue tropism.[9] Selective retargeting of PVLPs to specific cells can be achieved, for example, by genetic modification of capsids.[10,11] However, these modifications usually have an adverse effect on PVLP stability and substantially decrease particle production.[12−14]

Here, we describe retargeting of mouse PVLPs using surface protein chemical engineering. Mouse PVLPs are particularly interesting with respect to potential clinical use because of the absence of pre-existing immunity against mouse polyomaviruses in the human population. We hypothesized that creation of an array of bulky human transferrin (Tf) molecules on the PVLP surface could (i) create steric hindrance that would limit the undesirable nonspecific binding of VP1 to cell surfaces and (ii) target the newly engineered particles to cancer cells overexpressing the transferrin receptor (TfR). We utilized PVLPs based on mouse polyomavirus, which are composed of 72 pentameric subunits formed from 360 molecules of VP1 capsid protein. VP1 pentamers self-assemble into 45 nm empty viral capsids (PVLPs). These particles do not contain viral DNA and therefore are considered safe delivery vehicles.[5]

We expressed the VP1 protein in the baculovirus system, isolated the formed PVLPs as previously described,[15] and labeled them with rhodamine-NHS ester (providing PVLP* conjugate; see Figure 1) to allow fluorescence visualization. Then, we modified a part of PVLP* at the remaining lysines with an excess of a short PEG linker bearing a propargyl group (see Supporting Information for experimental details). We labeled human Tf with Alexa Fluor 488 and converted the 1,2-diols on sialic acid present in the Tf glycosylation pattern to aldehydes by mild periodate cleavage. We derivatized the obtained aldehydes with aminooxypropylazide, a "clickable" heterobifunctional linker that forms a physiologically stable aldoxime upon reaction with aldehyde (see Figure 1).[16] We then attached this Alexa Fluor 488-labeled Tf-azide conjugate (Tf*) to propargylated PVLP* via Cu(I)-catalyzed azide−alkyne cycloaddition (click chemistry),[17] obtaining PVLP-Tf* conjugate.

To characterize PVLP* and PVLP-Tf*, we confirmed the presence of Tf* on PVLP-Tf* by Western blot using antibodies against VP1 and Tf (Figure 2A and B) with

Received: October 27, 2016
Revised: December 28, 2016
Published: December 30, 2016

DOI: 10.1021/acs.bioconjchem.6b00622
Bioconjugate Chem. 2017, 28, 307−313

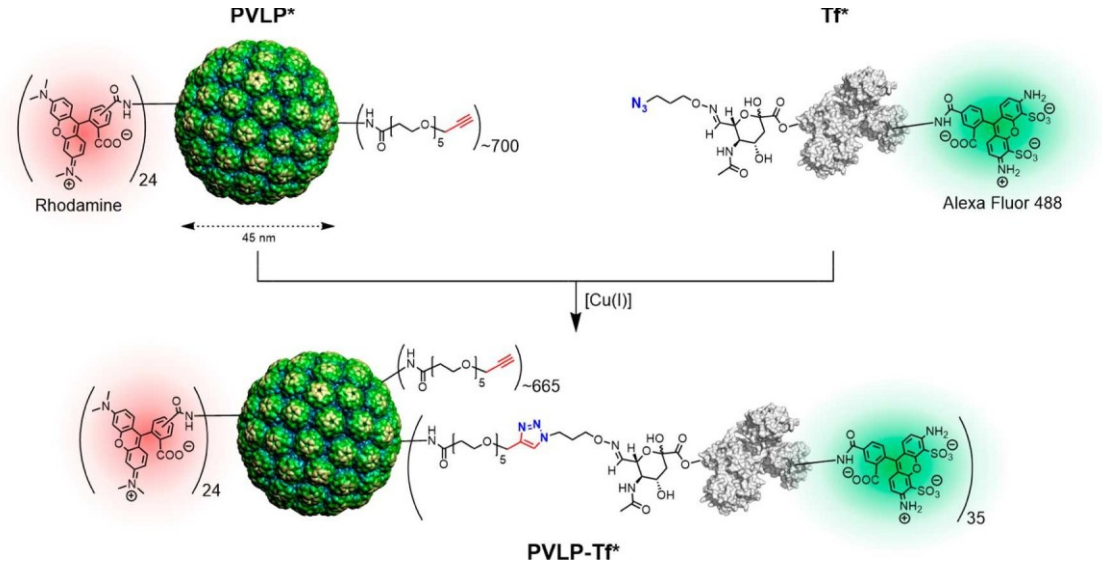

Figure 1. Schematic structure and preparation of PVLP* and PVLP-Tf* constructs. The source figure of PVLP was obtained from VIPERdb (http://viperdb.scripps.edu).[18]

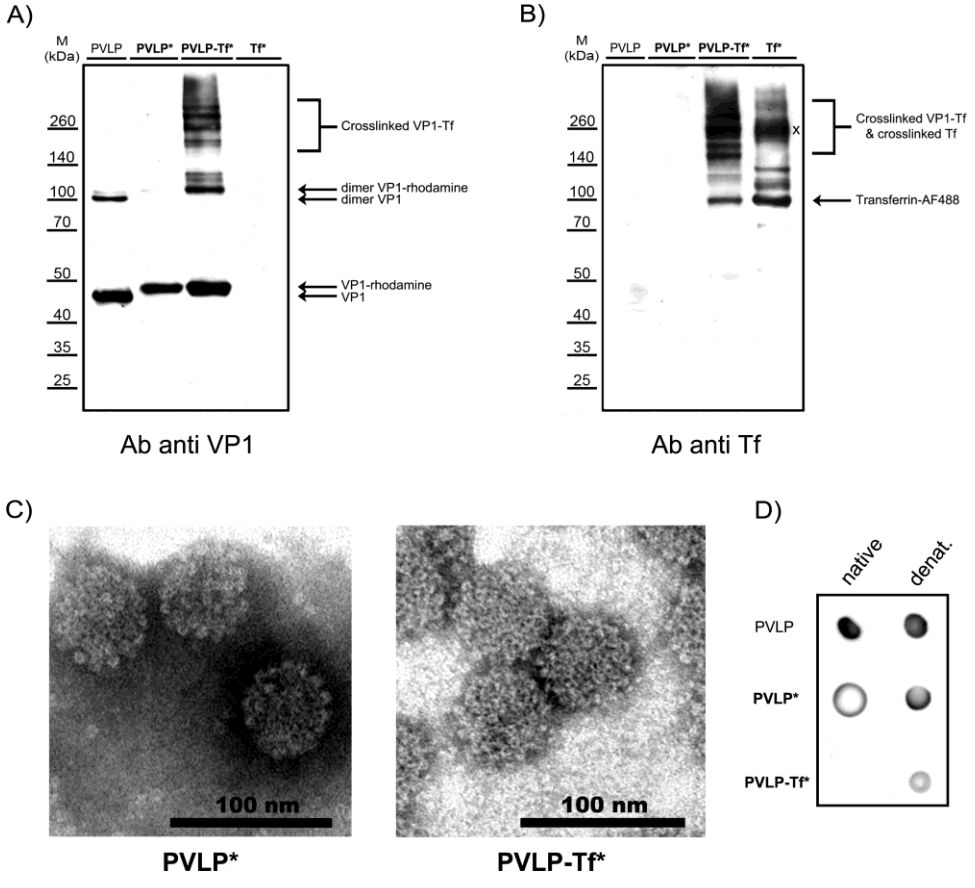

Figure 2. Characterization of PVLP* and PVLP-Tf* conjugates. Western blot analysis with antibody against VP1 protein (A) and antibody against Tf (B) after SDS-PAGE loaded with PVLP, PVLP*, PVLP-Tf*, and Tf*; the molecular weights are indicated on the left. The cross mark (×) represents cross-linked Tf* dimer. The other bands present in Tf* correspond to side products of Tf* modification and impurities contained in the starting Tf protein. (C) Transmission electron micrographs of PVLP* and PVLP-Tf* (negative staining). (D) Immunodot blot analysis of PVLP, PVLP*, and PVLP-Tf* probed with antibody against VP1. Native particles and particles denaturated by mercaptoethanol and heat (Laemli buffer, 100 °C) were dotted on the nitrocellulose membrane.

subsequent fluorescent detection (Figure S1A,B in Supporting Information). We identified both VP1 and Tf* in high molecular weight bands (>125 kDa) showing positive reaction with both antibodies. The presence of multiple bands containing VP1 and Tf* corresponds well to the aldoxime conjugation chemistry. Because the linkage used for Tf*

DOI: 10.1021/acs.bioconjchem.6b00622
Bioconjugate Chem. 2017, 28, 307−313

attachment is unstable under denaturing conditions, the PVLP-Tf* conjugate was partially cleaved to the original proteins. The observed high molecular weight bands most likely correspond to VP1 proteins cross-linked with multivalently azide-modified Tf* that were not disassembled during the denaturation procedure and to Tf* dimers (Figure 2A,B and Supporting Information Figure S1).

Transmission electron microscopy (TEM) confirmed the presence of intact monodispersed particles with a diameter of 55 ± 3 nm for PVLP* and 63 ± 4 nm for PVLP-Tf* (Figure 2C). Using dynamic light scattering (Figure S2 in Supporting Information), we ascertained that the particles do not aggregate and form a stable colloid. Their polydispersity indexes (0.15 and 0.12, respectively) refer to monodisperse particles.[19] Higher hydrodynamic diameter of PVLP-Tf* compared to PVLP* (68 and 59 nm, respectively) corresponds well to the result obtained from TEM. Considering the hydrodynamic diameter of Tf to be 7.4 nm,[20] the obtained values indicate deposition of Tf* in one layer, as expected for the engineered conjugation strategy. Extinction spectrum of PVLP-Tf* shows both characteristic absorption bands of rhodamine present in PVLP* and the Alexa Fluor 488 present in the attached Tf* (for spectra, see Figure S3 in Supporting Information).

For quantification of the Tf* load on PVLP-Tf*, we analyzed the concentration of the particles by Qubit protein assay and analyzed the Tf* loads using densitometric analysis on SDS-PAGE (Supporting Information Figure S1C). We obtained 35 ± 2 Tf*/PVLP-Tf* which provides ~24% surface coverage of PVLP-Tf* by Tf* (based on a simple spherical model approximating a PVLP* with a sphere of 45 nm diameter and Tf molecular footprint with a circle of 7.4 nm in diameter[20]). This coverage is comparable to that of previously prepared constructs of isosahedral VLPs bearing Tf[21−23] and corresponds to a local Tf* concentration of 0.44 mM in the volume constrained by the PVLP-Tf*.

We were further interested in whether the achieved surface density of Tf* on PVLP-Tf* can create the hypothesized steric hindrance to prevent interaction of VP1 with its targets. We performed immunodot blot analysis (Figure 2D) of VP1 protein and detected PVLP, PVLP*, and PVLP-Tf* using anti-VP1 antibody. Our anti-VP1 antibody provides dual selectivity, recognizing both the surface conformational epitope responsible for natural interaction with sialic acid in native particles and a C-terminal epitope that is accessible only in denatured PVLP.[24] While VP1 in native PVLP and PVLP* showed a positive reaction, recognition of VP1 in native PVLP-Tf* was completely abolished (Figure 2D). The presence of Tf* on PVLP-Tf* surface therefore prevents VP1-specific binding of native particles. Indeed, upon denaturation, the C-terminal epitope is exposed, and protein recognition by the anti-VP1 antibody is restored (Figure 2D).

Based on this finding, we analyzed the ability of PVLP-Tf* to selectively target TfR. This receptor is overexpressed and exposed on the membranes of numerous types of cancer cells, including pancreas, bladder, colon, lung, and breast cancers.[25−29] The elevated TfR expression correlates with cancer progression, tumor stage, and prognosis.[30,31] Interaction of Tf with TfR results in efficient clathrin-mediated endocytosis,[32] which can be used for selective delivery of Tf-modified molecules and particles to cancer cells.[33]

First, we analyzed the interaction of PVLP* and PVLP-Tf* with two human cancer cell lines, osteosarcoma cells (U2OS) and lymphoblastoid leukemia cells (CCRF-CEM), and one control, noncancerous human cell line represented by vein endothelial cells (HUVEC). We incubated these cells with particles (1×10^6 particles per cell; 0.54 nM particles; 1 h incubation in serum-free media), washed them twice with PBS, and analyzed the cells using flow cytometry. To confirm binding selectivity, we blocked the TfR on cells using a high concentration of free Tf (negative control, Tf+PVLP-Tf*). For both cancer cell lines, we observed extremely high levels of PVLP-Tf* uptake, whereas the negative controls performed after saturation of TfR by free Tf showed negligible interaction (Figure 3 and Supporting Information Figure S4). U2OS and CCRF-CEM cells showed relative fluorescence intensities 50 and 120 times higher than those of the negative controls, respectively. This finding is consistent with the previously observed higher expression of TfR in osteosarcoma and lymphoblastoid leukemia.[34,35] HUVEC, like all mammalian cells, also display TfR, but to a much lower extent. Correspondingly, we observed a weak, but selective binding of PVLP-Tf* to these cells, which can be similarly blocked with free Tf (Figure 3). In summary, these data indicate (i) high affinity of PVLP-Tf* to cancer cells and (ii) high selectivity of its binding to the TfR.

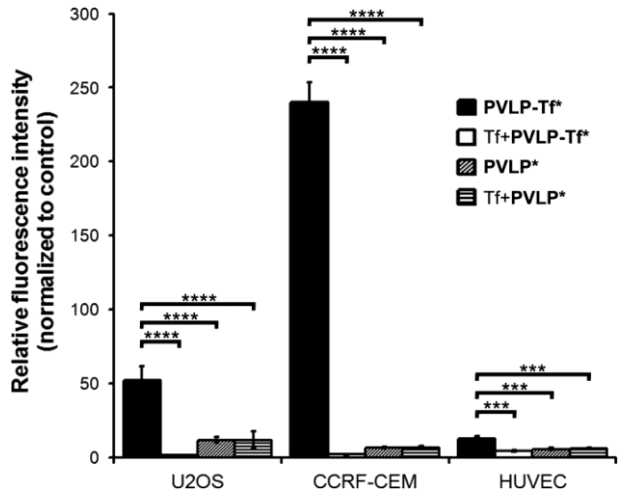

Figure 3. Flow cytometry study of PVLP-Tf* and PVLP* association with U2OS, CCRF-CEM, and HUVEC cells. The cells were subjected to particles with (Tf+) or without preincubation with free Tf. Data represent fluorescence normalized against autofluorescence from control cells with standard deviations calculated from quadruplicates (two independent experiments in duplicates). There was a statistically significant difference between the PVLP-Tf* variant and the controls. All other comparisons were not significant (one-way ANOVA followed by Tukey's posthoc test). ***$p < 0.001$. ****$p < 0.0001$.

Furthermore, we analyzed the interaction of PVLP* with cells under the same conditions. In contrast to PVLP-Tf*, the PVLP* particles retained their capacity to bind the cells in VP1-specific manner (Figure 3). This interaction is clearly not related to the TfR, because the binding did not significantly change in the presence or absence of free Tf (compare PVLP* and Tf+PVLP*). Based on these data and on our immunodot blot analysis (Figure 2D), we conclude that installation of sterically demanding Tf* molecules on the PVLP surface can suppress the VP1-specific binding of the particles. Because PVLP* binds readily to cells and interact with the anti-VP1 antibody, whereas PVLP-Tf* binds specifically to TfR and do not interact with the anti-VP1 antibody, we suggest that Tf*

DOI: 10.1021/acs.bioconjchem.6b00622
Bioconjugate Chem. 2017, 28, 307−313

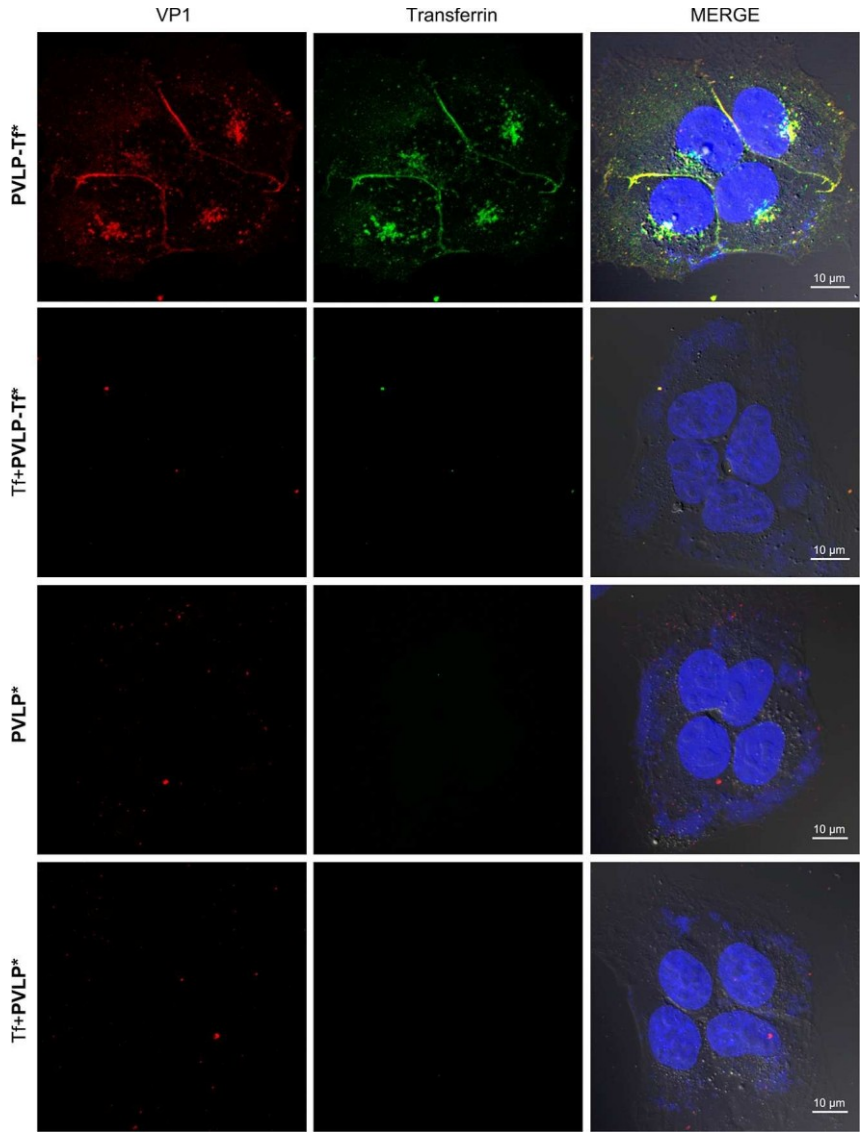

Figure 4. Confocal microscopy study of PVLP-Tf* and PVLP* uptake by U2OS cells. The cells were treated for 1 h with particles with (Tf+) or without preincubation with free Tf (30 min) and fixed. Confocal sections of representative cells with corresponding signal in green (Tf conjugated with Alexa Fluor 488 in PVLP-Tf*) or red (VP1 conjugated with rhodamine in PVLP* and PVLP-Tf*) channels are shown. Nuclei are shown in blue (DAPI). Merge is composed of all three channels and bright field image. The images are shown as a maximum intensity Z-projection.

sterically blocks the conformational epitope responsible for the natural VP1-specific cell surface binding of PVLPs.

To visualize the interaction of PVLP-Tf* and PVLP* particles with cells, we used confocal microscopy on fixed U2OS cells. The incubation conditions were similar to the flow cytometry experiments (1 h incubation in serum-free media, Tf+ as a negative control). We observed strong binding of PVLP-Tf* to the cells, which can be completely blocked by free Tf (Figure 4). In contrast, the binding of PVLP* was negligible in the presence or absence of Tf. These results are consistent with the flow cytometry experiments and further corroborate the selectivity and effectivity of the uptake.

We observed fast internalization of PVLP-Tf*. Only 1 h after exposing cells to the particles, we found a significant fraction of particles near nuclei in a pericentriolar area that likely represents the recycling compartment, the site of accumulation of rapidly endocyted transferrin (Supporting Information Figure S5).[36,37] Although polyomavirus naturally accumulates in the perinuclear space[38] and meets the transferrin during the endocytic pathway in recycling endosomes 3 h post infection,[39,40] the fast accumulation of PVLP-Tf* in this region likely indicates that PVLP-Tf* were targeted to TfR. To avoid potential artifacts related to cell fixation, we repeated these experiments also with live cells. Both approaches did not show a difference in intracellular distribution of particles (Supporting Information Figure S6).

Finally, we utilized the presence of two fluorescent labels on the PVLP-Tf* conjugate (Alexa Fluor 488 on Tf* and rhodamine on VP1). Using colocalization analysis (see Supporting Information for details), we studied whether Tf* dissociates from the PVLP-Tf* conjugate or remains bound on VP1 protein. Based on the high Manders colocalization coefficient values (0.747; 0.724), we conclude that the linkages generated by the used conjugation chemistry are stable during the experiment and Tf* molecules do not detach from VP1 inside the cells.

Overall, our results indicate that PVLP can be efficiently retargeted using surface attachment of Tf, expanding the family

DOI: 10.1021/acs.bioconjchem.6b00622
Bioconjugate Chem. 2017, 28, 307−313

of VLPs that can operate in a similar way in numerous types of cancer cell lines. These include VLPs based on Brome mosaic virus,[21] adenovirus,[41−43] and various bacteriophages.[22,23,44−47] The PVLP-Tf* conjugates show notably high uptake, especially to leukemia CCRF-CEM cells (up to 120-fold compared to the control). To the best of our knowledge, comparably high values have not been documented to date for any other cell line and VLP. However, direct comparison with previously described constructs is often difficult, because of different approaches used for their evaluation (involving functional assays such as cell killing,[45,47] and the reporter gene expression[41]).

Several factors may contribute to the high targeting efficacy of PVLP-Tf*. We emphasize the importance of the local attachment geometry of Tf*, which is related to the attachment chemistry. For example, nonspecific amide-based bioconjugation via lysines on VLP[41,48] produces a statistical orientation of protein on the surface and correspondingly low recognition rate by TfR. On the other hand, selective conjugation via a well- defined and properly oriented position can overcome this problem.[21,22,44,46] For Tf* attachment, we utilized the molecularly defined glycosidation pattern, which can be selectively transformed to a "clickable" moiety (Figure 1) and ligated to a VLP using Cu-catalyzed azide−alkyne cycloaddition (click chemistry).[23] This conjugation approach provides a high degree of flexibility of Tf* attached to a particle and a preferential Tf* orientation for interaction with TfR. Furthermore, the avidity caused by the high local concentration of Tf* (0.44 mM) contributes to the enhanced targeting effect.

The crucial feature in nanoparticulate drug delivery is assembly/disassembly behavior, which has been pioneered for VLPs in the early 1990s[48,49] and successfully demonstrated for Tf-based targeted delivery of siRNA by bacteriophage MS2 synthetic virions.[45,47] Based on previously demonstrated assembly/disassembly of PVLPs and their functional use as nanocontainers for delivery and release of nucleic acids,[5,6] one can expect the similar advantage also for PVLP-Tf*. We thus believe that PVLP-Tf* can become a modular and effective platform for VLP-based drug delivery devices.

In summary, we demonstrated that mouse PVLPs can be retargeted from their natural sialic acid receptor to leukemia and osteosarcoma cells by engineering an array of 35 ± 2 Tf* molecules on the surface of each particle. The surface architecture, type of Tf chemical modification, and ligation approach we used resulted in a particularly strong and selective interaction of the PVLP-Tf* conjugate with cells. Moreover, the modification with Tf* clearly rid PVLP of undesirable ubiquitous binding to cells. Based on immunodot blot analysis and competitive cellular binding experiments, we suggest that the surface-bound Tf* blocks the surface conformational epitope on PVLP responsible for natural interaction with sialic acid. Although the competitive impact of blood Tf and protein corona on Tf-based targeting has been recently demonstrated,[50] we believe that the strong avidity effects on PVLP-Tf* binding combined with the binding selectivity can lead to efficient in vivo targeting of tumors. We are currently working along these lines, aiming for delivery of therapeutic and/or diagnostic molecules using this system.

ASSOCIATED CONTENT

Supporting Information

The Supporting Information is available free of charge on the ACS Publications website at DOI: 10.1021/acs.bioconjchem.6b00622.

Experimental procedures; electrophoretic, spectral, and light scattering characterization of PVLP particles; source data for flow cytometry experiments; additional images from confocal microscopy (PDF)

AUTHOR INFORMATION

Corresponding Author

*E-mail: cigler@uochb.cas.cz.

ORCID

Petr Cigler: 0000-0003-0283-647X

Notes

The authors declare no competing financial interest.

ACKNOWLEDGMENTS

This work was supported by the League Against Cancer Prague (J.Z.S., H.S., J.F.), the SVV-2016-260314 (J.Z.S), the Grant Agency of Charles University (project no. 727816, J.N., P.C.), and European Regional Development Fund and the state budget of the Czech Republic, project no. CZ.1.05/4.1.00/16.0347 (confocal microscope Zeiss LSM 880). The authors are grateful to Miroslav Hajek, Lukas Hejtmanek, and Alzbeta Sekavova for their valuable help.

ABBREVIATIONS USED

CCRF-CEM, lymphoblastoid leukemia cell line; HUVEC, human umbilical vein endothelial cells; PBS, phosphate buffered saline; PEG, poly(ethylene glycol); PVLP, polyomavirus-like particles; U2OS, human osteosarcoma cell line; VLP, virus-like particle; VP1, major coat protein; TEM, transmission electron microscopy; Tf, transferrin; TfR, transferrin receptor

REFERENCES

(1) Steinmetz, N. F. (2010) Viral nanoparticles as platforms for next-generation therapeutics and imaging devices. *Nanomedicine 6*, 634−641.

(2) Strable, E., and Finn, M. G. (2009) Chemical modification of viruses and virus-like particles. *Curr. Top. Microbiol. Immunol. 327*, 1−21.

(3) Suchanova, J., Spanielova, H., and Forstova, J. (2015) Applications of Viral Nanoparticles Based on Polyomavirus and Papillomavirus Structures, in *Viral Nanotechnology*, pp 303−362, CRC Press.

(4) Teunissen, E. A., de Raad, M., and Mastrobattista, E. (2013) Production and biomedical applications of virus-like particles derived from polyomaviruses. *J. Controlled Release 172*, 305−321.

(5) Forstova, J., Krauzewicz, N., Sandig, V., Elliott, J., Palkova, Z., Strauss, M., and Griffin, B. E. (1995) Polyoma virus pseudocapsids as efficient carriers of heterologous DNA into mammalian cells. *Hum. Gene Ther. 6*, 297−306.

(6) Kler, S., Asor, R., Li, C., Ginsburg, A., Harries, D., Oppenheim, A., Zlotnick, A., and Raviv, U. (2012) RNA encapsidation by SV40-derived nanoparticles follows a rapid two-state mechanism. *J. Am. Chem. Soc. 134*, 8823−8830.

(7) Li, F., Zhang, Z.-P., Peng, J., Cui, Z.-Q., Pang, D.-W., Li, K., Wei, H.-P., Zhou, Y.-F., Wen, J.-K., and Zhang, X.-E. (2009) Imaging Viral Behavior in Mammalian Cells with Self-Assembled Capsid-Quantum-Dot Hybrid Particles. *Small 5*, 718−726.

(8) Enomoto, T., Kawano, M., Fukuda, H., Sawada, W., Inoue, T., Haw, K. C., Kita, Y., Sakamoto, S., Yamaguchi, Y., Imai, T., et al. (2013) Viral protein-coating of magnetic nanoparticles using simian virus 40 VP1. *J. Biotechnol. 167*, 8−15.

(9) Krauzewicz, N., Cox, C., Soeda, E., Clark, B., Rayner, S., and Griffin, B. E. (2000) Sustained ex vivo and in vivo transfer of a reporter gene using polyoma virus pseudocapsids. *Gene Ther. 7*, 1094−1102.

(10) Inoue, T., Kawano, M., Takahashi, R., Tsukamoto, H., Enomoto, T., Imai, T., Kataoka, K., and Handa, H. (2008) Engineering of SV40-based nano-capsules for delivery of heterologous proteins as fusions with the minor capsid proteins VP2/3. *J. Biotechnol. 134*, 181−192.
(11) Abbing, A., Blaschke, U. K., Grein, S., Kretschmar, M., Stark, C. M. B., Thies, M. J. W., Walter, J., Weigand, M., Woith, D. C., Hess, J., et al. (2004) Efficient intracellular delivery of a protein and a low molecular weight substance via recombinant polyomavirus-like particles. *J. Biol. Chem. 279*, 27410−27421.
(12) Takahashi, R., Kanesashi, S., Inoue, T., Enomoto, T., Kawano, M., Tsukamoto, H., Takeshita, F., Imai, T., Ochiya, T., Kataoka, K., et al. (2008) Presentation of functional foreign peptides on the surface of SV40 virus-like particles. *J. Biotechnol. 135*, 385−392.
(13) Langner, J., Neumann, B., Goodman, S. L., and Pawlita, M. (2004) RGD-mutants of B-lymphotropic polyomavirus capsids specifically bind to αvβ3 integrin. *Arch. Virol. 149*, 1877−1896.
(14) Shin, Y. C., and Folk, W. R. (2003) Formation of Polyomavirus-Like Particles with Different VP1Molecules That Bind the Urokinase Plasminogen Activator Receptor. *J. Virol. 77*, 11491−11498.
(15) Forstova, J., Krauzewicz, N., Wallace, S., Street, A. J., Dilworth, S. M., Beard, S., and Griffin, B. E. (1993) Cooperation of structural proteins during late events in the life cycle of polyomavirus. *J. Virol. 67*, 1405−1413.
(16) Rehor, I., Lee, K. L., Chen, K., Hajek, M., Havlik, J., Lokajova, J., Masat, M., Slegerova, J., Shukla, S., Heidari, H., et al. (2015) Plasmonic nanodiamonds: targeted core−shell type nanoparticles for cancer cell thermoablation. *Adv. Healthcare Mater. 4*, 460−468.
(17) Presolski, S. I., Hong, V. P., and Finn, M. G. (2011) Copper-Catalyzed Azide-Alkyne Click Chemistry for Bioconjugation, in *Current Protocols in Chemical Biology* (Arkin, A. P., Mahal, L., Romesberg, F., Shah, K., Shamu, C., and Thomas, C., Eds.) John Wiley & Sons, Inc., Hoboken, NJ, USA.
(18) Carrillo-Tripp, M., Shepherd, C. M., Borelli, I. A., Venkataraman, S., Lander, G., Natarajan, P., Johnson, J. E., Brooks, C. L., and Reddy, V. S. (2009) VIPERdb2: an enhanced and web API enabled relational database for structural virology. *Nucleic Acids Res. 37*, D436−D442.
(19) Khurshid, S., Saridakis, E., Govada, L., and Chayen, N. E. (2014) Porous nucleating agents for protein crystallization. *Nat. Protoc. 9*, 1621−1633.
(20) Armstrong, J. K., Wenby, R. B., Meiselman, H. J., and Fisher, T. C. (2004) The Hydrodynamic Radii of Macromolecules and Their Effect on Red Blood Cell Aggregation. *Biophys. J. 87*, 4259−4270.
(21) Yildiz, I., Tsvetkova, I., Wen, A. M., Shukla, S., Masarapu, M. H., Dragnea, B., and Steinmetz, N. F. (2012) Engineering of Brome mosaic virus for biomedical applications. *RSC Adv. 2*, 3670.
(22) Huang, R. K., Steinmetz, N. F., Fu, C.-Y., Manchester, M., and Johnson, J. E. (2011) Transferrin-mediated targeting of bacteriophage HK97 nanoparticles into tumor cells. *Nanomedicine 6*, 55−68.
(23) Banerjee, D., Liu, A. P., Voss, N. R., Schmid, S. L., and Finn, M. G. (2010) Multivalent Display and Receptor-Mediated Endocytosis of Transferrin on Virus-Like Particles. *ChemBioChem 11*, 1273−1279.
(24) Stehle, T., and Harrison, S. C. (1996) Crystal structures of murine polyomavirus in complex with straight-chain and branched-chain sialyloligosaccharide receptor fragments. *Structure 4*, 183−194.
(25) Ryschich, E., Huszty, G., Knaebel, H. P., Hartel, M., Büchler, M. W., and Schmidt, J. (2004) Transferrin receptor is a marker of malignant phenotype in human pancreatic cancer and in neuroendocrine carcinoma of the pancreas. *Eur. J. Cancer 40*, 1418−1422.
(26) Seymour, G. J., Walsh, M. D., Lavin, M. F., Strutton, G., and Gardiner, R. A. (1987) Transferrin receptor expression by human bladder transitional cell carcinomas. *Urol. Res. 15*, 341−344.
(27) Prutki, M., Poljak-Blazi, M., Jakopovic, M., Tomas, D., Stipancic, I., and Zarkovic, N. (2006) Altered iron metabolism, transferrin receptor 1 and ferritin in patients with colon cancer. *Cancer Lett. 238*, 188−196.
(28) Kondo, K., Noguchi, M., Mukai, K., Matsuno, Y., Sato, Y., Shimosato, Y., and Monden, Y. (1990) Transferrin receptor expression in adenocarcinoma of the lung as a histopathologic indicator of prognosis. *Chest 97*, 1367−1371.
(29) Walker, R. A., and Day, S. J. (1986) Transferrin receptor expression in non-malignant and malignant human breast tissue. *J. Pathol. 148*, 217−224.
(30) Prior, R., Reifenberger, G., and Wechsler, W. (1990) Transferrin receptor expression in tumours of the human nervous system: relation to tumour type, grading and tumour growth fraction. *Virchows Arch. A: Pathol. Anat. Histopathol. 416*, 491−496.
(31) Daniels, T. R., Delgado, T., Rodriguez, J. A., Helguera, G., and Penichet, M. L. (2006) The transferrin receptor part I: Biology and targeting with cytotoxic antibodies for the treatment of cancer. *Clin. Immunol. 121*, 144−158.
(32) Dautry-Varsat, A. (1986) Receptor-mediated endocytosis: the intracellular journey of transferrin and its receptor. *Biochimie 68*, 375−381.
(33) Daniels, T. R., Bernabeu, E., Rodríguez, J. A., Patel, S., Kozman, M., Chiappetta, D. A., Holler, E., Ljubimova, J. Y., Helguera, G., and Penichet, M. L. (2012) The transferrin receptor and the targeted delivery of therapeutic agents against cancer. *Biochim. Biophys. Acta, Gen. Subj. 1820*, 291−317.
(34) Nakase, M., Inui, M., Okumura, K., Kamei, T., Nakamura, S., and Tagawa, T. (2005) p53 gene therapy of human osteosarcoma using a transferrin-modified cationic liposome. *Mol. Cancer Ther. 4*, 625−631.
(35) Petrini, M., Pelosi-Testa, E., Sposi, N. M., Mastroberardino, G., Camagna, A., Bottero, L., Mavilio, F., Testa, U., and Peschle, C. (1989) Constitutive expression and abnormal glycosylation of transferrin receptor in acute T-cell leukemia. *Cancer Res. 49*, 6989−6996.
(36) Ren, M., Xu, G., Zeng, J., De Lemos-Chiarandini, C., Adesnik, M., and Sabatini, D. D. (1998) Hydrolysis of GTP on rab11 is required for the direct delivery of transferrin from the pericentriolar recycling compartment to the cell surface but not from sorting endosomes. *Proc. Natl. Acad. Sci. U. S. A. 95*, 6187−6192.
(37) Ullrich, O., Reinsch, S., Urbe, S., Zerial, M., and Parton, R. G. (1996) Rab11 regulates recycling through the pericentriolar recycling endosome. *J. Cell Biol. 135*, 913−924.
(38) Richterova, Z., Liebl, D., Horak, M., Palkova, Z., Stokrova, J., Hozak, P., Korb, J., and Forstova, J. (2001) Caveolae Are Involved in the Trafficking of Mouse Polyomavirus Virions and Artificial VP1 Pseudocapsids toward Cell Nuclei. *J. Virol. 75*, 10880−10891.
(39) Mannova, P., and Forstova, J. (2003) Mouse Polyomavirus Utilizes Recycling Endosomes for a Traffic Pathway Independent of COPI Vesicle Transport. *J. Virol. 77*, 1672−1681.
(40) Liebl, D., Difato, F., Hornikova, L., Mannova, P., Stokrova, J., and Forstova, J. (2006) Mouse Polyomavirus Enters Early Endosomes, Requires Their Acidic pH for Productive Infection, and Meets Transferrin Cargo in Rab11-Positive Endosomes. *J. Virol. 80*, 4610−4622.
(41) Kreppel, F., Gackowski, J., Schmidt, E., and Kochanek, S. (2005) Combined Genetic and Chemical Capsid Modifications Enable Flexible and Efficient De- and Retargeting of Adenovirus Vectors. *Mol. Ther. 12*, 107−117.
(42) Campos, S. (2004) Avidin-based targeting and purification of a protein IX-modified, metabolically biotinylated adenoviral vector. *Mol. Ther. 9*, 942−954.
(43) Oh, K. S., Engler, J. A., and Joung, I. (2005) Enhancement of gene delivery to cancer cells by a retargeted adenovirus. *J. Microbiol. 43*, 179−182.
(44) Khalaj-Kondori, M., Kavoosi, M., Rahmati-Yamchi, M., and Kadivar, M. (2016) Preparation of a transferrin-targeted M13-based gene nanocarrier and evaluation of its efficacy for gene delivery and expression in eukaryote cells. *Turk. J. Biol. 40*, 561−570.
(45) Galaway, F. A., and Stockley, P. G. (2013) MS2 Viruslike Particles: A Robust, Semisynthetic Targeted Drug Delivery Platform. *Mol. Pharmaceutics 10*, 59−68.
(46) Khalaj-Kondori, M., Sadeghizadeh, M., Behmanesh, M., Saggio, I., and Monaci, P. (2011) Chemical coupling as a potent strategy for preparation of targeted bacteriophage-derived gene nanocarriers into

DOI: 10.1021/acs.bioconjchem.6b00622
Bioconjugate Chem. 2017, 28, 307−313

eukaryotic cells: Chemically targeted bacteriophage-derived gene nanocarriers. *J. Gene Med. 13*, 622−631.

(47) Wu, M., Sherwin, T., Brown, W. L., and Stockley, P. G. (2005) Delivery of antisense oligonucleotides to leukemia cells by RNA bacteriophage capsids. *Nanomedicine 1*, 67−76.

(48) Wu, M., Brown, W. L., and Stockley, P. G. (1995) Cell-specific delivery of bacteriophage-encapsidated ricin A chain. *Bioconjugate Chem. 6*, 587−595.

(49) Mastico, R. A., Talbot, S. J., and Stockley, P. G. (1993) Multiple presentation of foreign peptides on the surface of an RNA-free spherical bacteriophage capsid. *J. Gen. Virol. 74*, 541−548.

(50) Salvati, A., Pitek, A. S., Monopoli, M. P., Prapainop, K., Bombelli, F. B., Hristov, D. R., Kelly, P. M., Åberg, C., Mahon, E., and Dawson, K. A. (2013) Transferrin-functionalized nanoparticles lose their targeting capabilities when a biomolecule corona adsorbs on the surface. *Nat. Nanotechnol. 8*, 137−143.

DOI: 10.1021/acs.bioconjchem.6b00622
Bioconjugate Chem. 2017, 28, 307−313